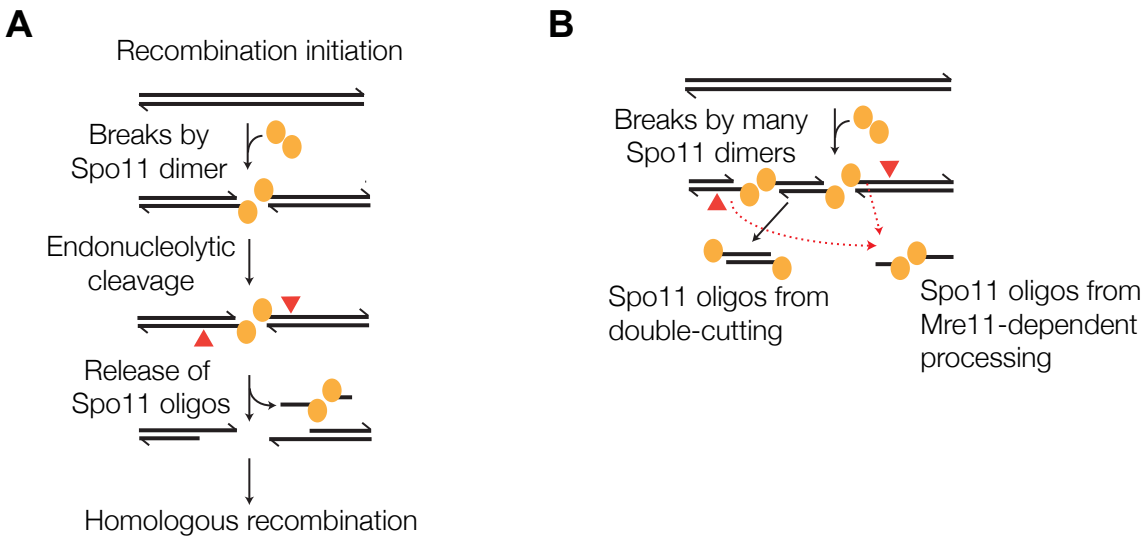

Supplemental Fig. S1. Schematic of recombination initiation pathway.
(*A*) Normal DSB formation and processing. Parallel black lines represent the two strands of double-stranded DNA with arrowheads indicating the 3′ ends. A dimer of Spo11 (yellow ovals) cleaves both strands of the DNA molecule, remaining attached to the 5′ ends of the DSB. Spo11 is released following Mre11-dependent endonucleolytic cleavage (red triangles) of the strands to which Spo11 is attached. (*B*) Model for Mre11-independent generation of Spo11 oligos via formation of adjacent DSBs.

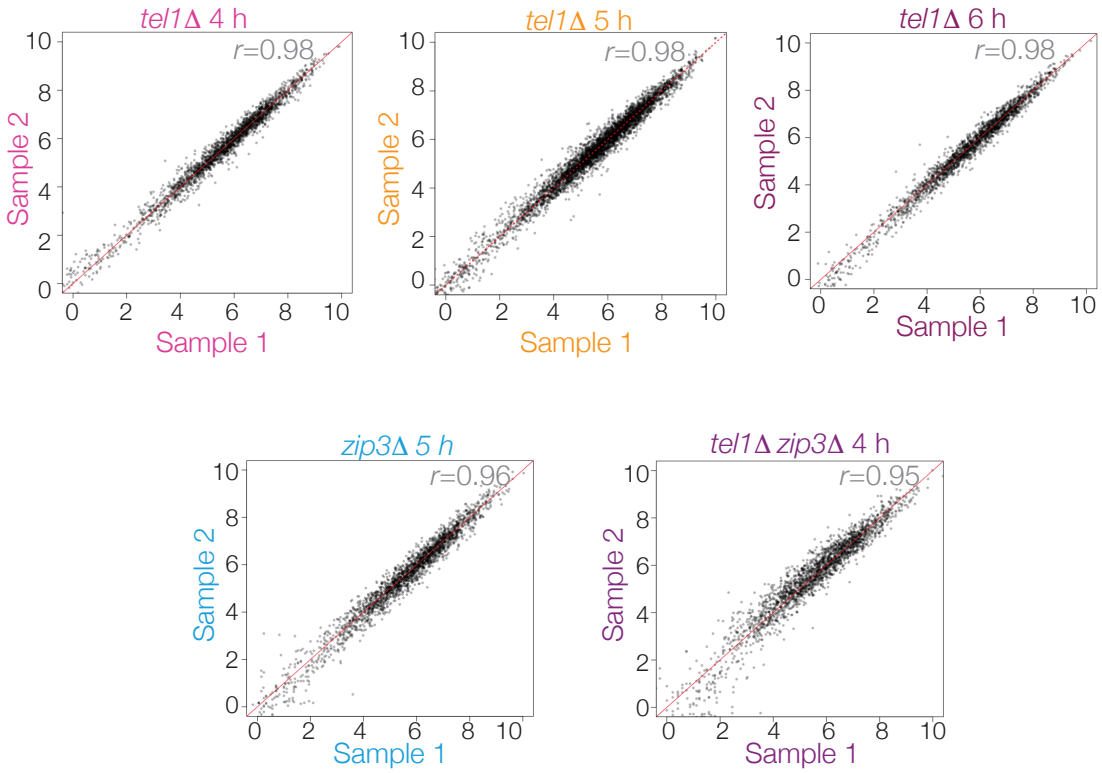

Supplemental Fig. S2. Reproducibility of Spo11-oligo maps.
Each point shows the sum of Spo11 oligos ($\log_2$) in 5-kb non-overlapping bins across the genome. Biological replicate samples are compared for each genotype and time point indicated. For subsequent analyses, the replicate samples were averaged. Pearson's correlation coefficients are shown on the top right. Diagonal red lines have a slope of 1. The *zip3Δ* samples are from (Thacker et al. 2014) and were collected at 5 h in meiosis.

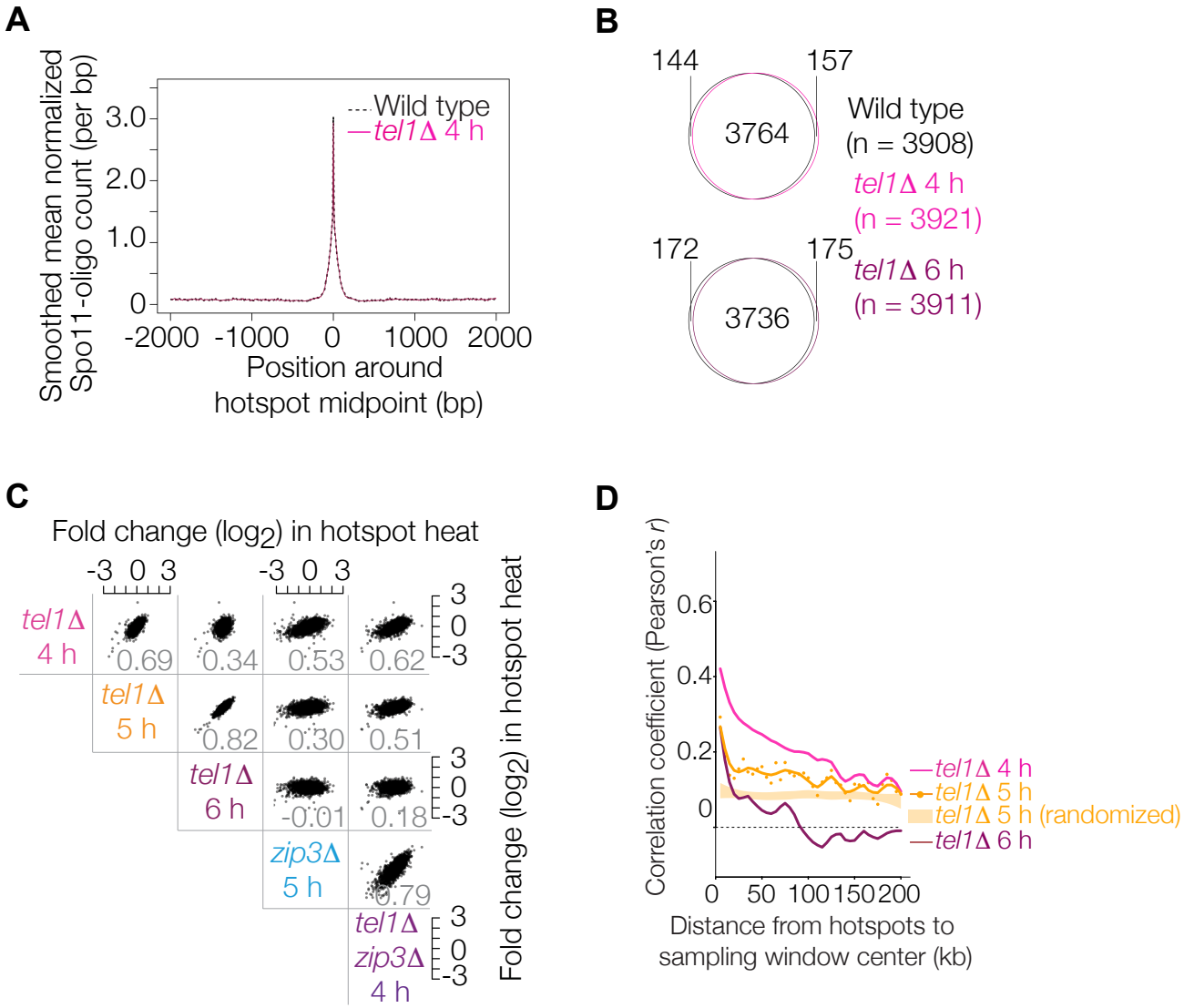

Supplemental Fig. S3. Hotspot-level effects of the *tel1Δ* mutation.
(*A*) Hotspot widths are unaltered in *tel1Δ*. Spo11 oligos (normalized to RPM) were smoothed with a 201-bp Hann window and averaged around 3908 hotpots as defined in an averge Spo11-oligo map compiled from multiple wild-type datasets (see Methods). Identical results were obtained with the *tel1Δ* 6-h dataset. (*B*) Venn diagrams depicting the high degree of overlap between hotspots called in wild-type and *tel1Δ* Spo11-oligo maps. (*C*) Comparison between mutants for changes in activity of individual hotspots. Each point displays the pairwise comparison between mutant datasets for the fold change ($\log_2$, relative to wild type) in Spo11-oligo counts within a hotspot. Correlation coefficients (Pearson's *r*) are shown at lower right of each plot. *(D)* Local domains of correlated behavior (as in Fig. 4D). Data for *tel1Δ* at 4 h and 6 h are reproduced from Fig. 4D.

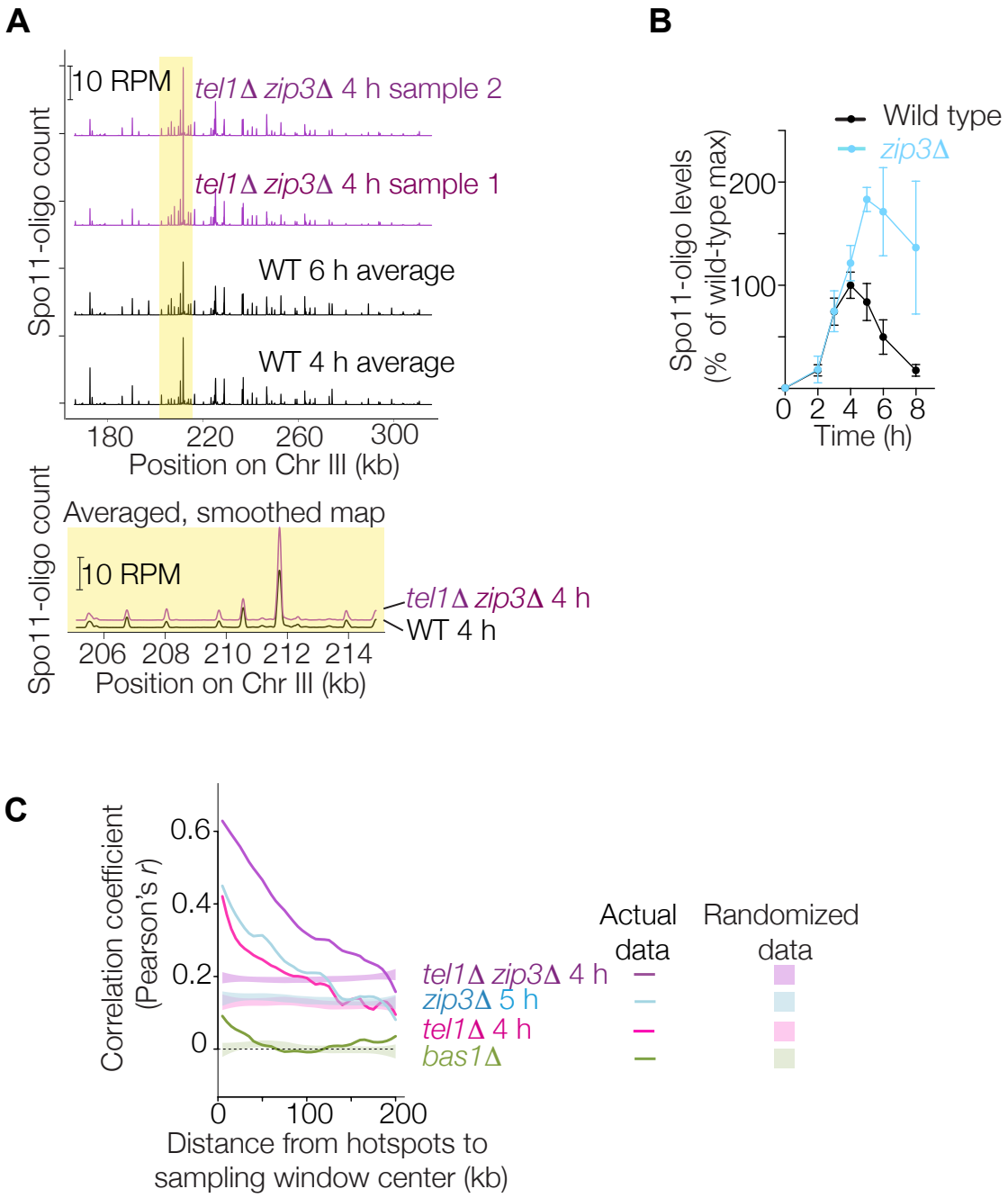

Supplemental Fig. S4. Spo11-oligo landscape in the *tel1Δ zip3Δ* double mutant. (*A*) Reproducibility of Spo11-oligo maps. A representative genomic segment is shown as in Fig. 4A. (*B*) Spo11-oligo quantification for the *zip3Δ* single mutant reproduced from (Thacker et al. 2014). (*C*) Local domains of correlated behavior. The data from Fig. 5B are reproduced along with 95% confidence intervals for data randomized within-chromosome. For clarity, only the local regression lines fitted to the real data and not the individual points are shown.

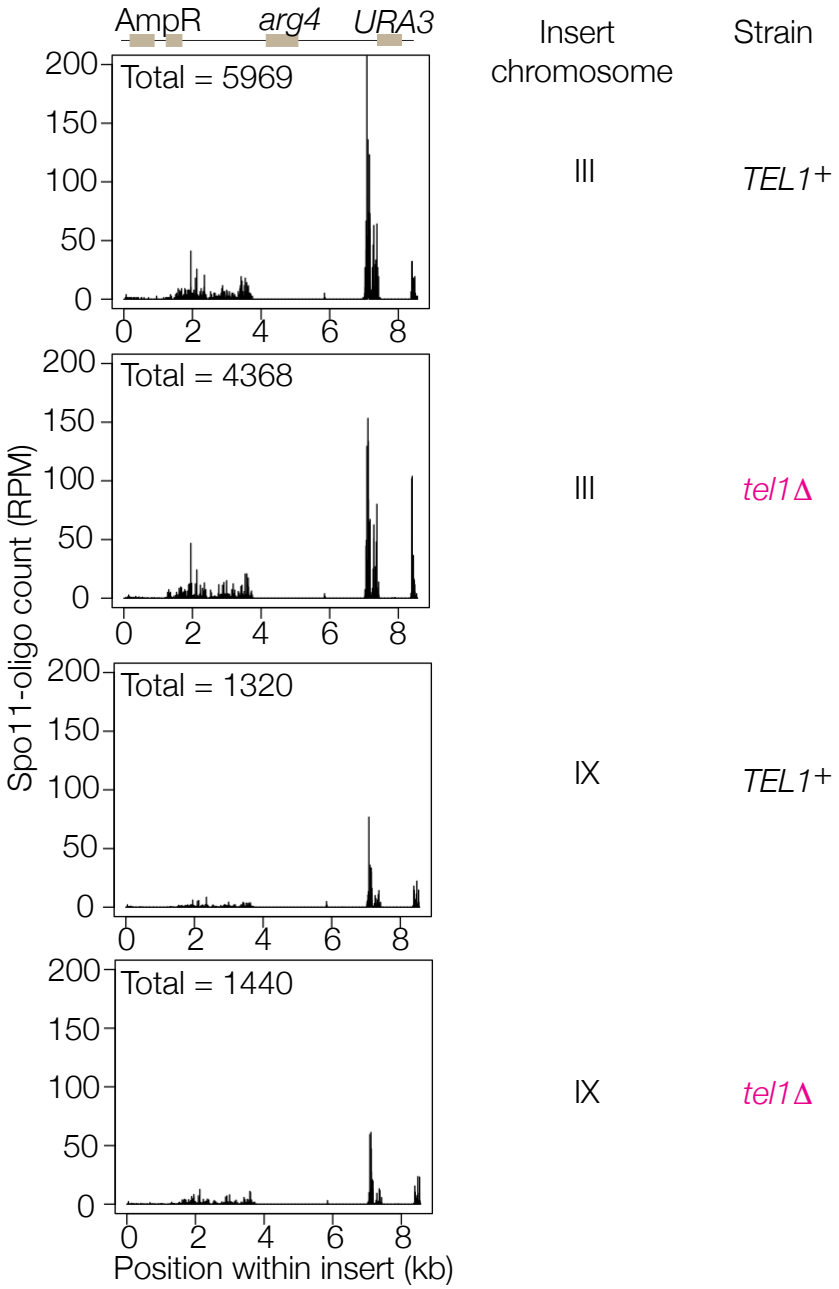

Supplemental Fig. S5. Uniquely mapping Spo11 oligos within the artificial hotspot insert. A schematic of the artificial hotspot insert bearing mutant *arg4* and wild-type *URA3* genes within plasmid sequences is shown at upper left (Wu and Lichten 1995). Normalized unique Spo11-oligo maps within the insert are shown for the indicated *TEL*1 genotypes and insert positions. Total normalized Spo11-oligo counts (RPM) are indicated at upper left of each plot. Note that DSBs form principally within the plasmid backbone, as previously described (Wu and Lichten 1995). Spo11-oligo maps across the insert can be found in Supplemental Table S4.

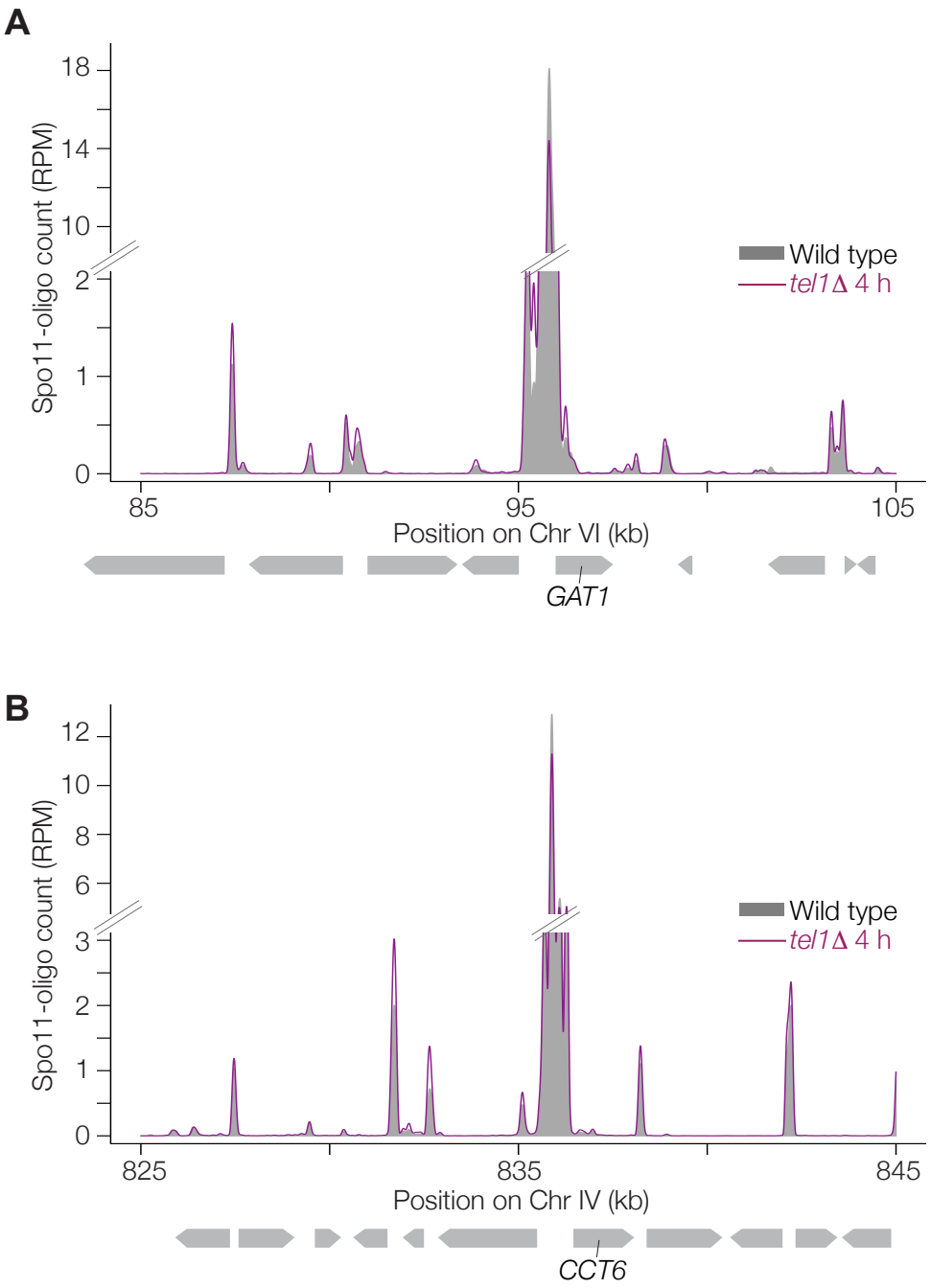

Supplemental Fig. S6. Regions around strong natural hotspots.
Spo11-oligo profiles around the *GAT1* (panel *A*) and *CCT6* (panel *B*) hotspots. Data were smoothed with a 201-bp Hann sliding window. Data are plotted as RPM without scaling to account for the overall increase in Spo11-oligo levels in *tel1Δ*; this allows the comparison between *tel1Δ* and wild type to provide a direct visualization of changes in hotspot activity relative to the genome average.

Table S1. Spo11-oligo mapping statistics.

Dataset	Total sequenced	Total mapped[a]	Total filtered[b]	Uniquely mapped to sacCer2[c]
Wild type 4 h sample 1	4,533,876	2,791,337 (61.6%)	ND	2,333,272 (51.5%)
Wild type 4 h sample 2	9,370,434	9,309,330 (99.3%)	7,825,295 (83.5%)	7,601,170 (81.1%)
Wild type 5 h sample 1	9,155,328	8,876,358 (97.0%)	7,374,704 (81.0%)	7,198,251 (78.6%)
Wild type 5 h sample 2	6,894,780	6,855,232 (99.4%)	5,844,523 (84.8%)	5,736,908 (83.2%)
Wild type 6 h sample 1	11,775,326	11,335,086 (96.3%)	8,790,160 (74.6%)	8,431,705 (71.6%)
Wild type 6 h sample 2	7,331,757	6,960,685 (94.9%)	5,817,567 (79.3%)	5,661,799 (77.2%)
*tel1*Δ 4 h sample 1	15,107,826	14,676,572 (97.1%)	13,050,426 (86.4%)	12,808,721 (84.8%)
*tel1*Δ 4 h sample 2	9,481,848	9,447,759 (99.7%)	8,540,258 (90.1%)	8,373,653 (88.3%)
*tel1*Δ 5 h sample 1	9,063,352	9,023,209 (99.6%)	8,137,106 (89.8%)	7,994,294 (88.2%)
*tel1*Δ 5 h sample 2	11,757,896	11,706,818 (99.6%)	10,586,665 (90.0%)	10,373,535 (88.2%)
*tel1*Δ 6 h sample 1	12,034,357	11,972,534 (99.5%)	10,736,079 (89.2%)	10,551,936 (87.7%)
*tel1*Δ 6 h sample 2	8,523,723	8,501,360 (99.7%)	7,684,531 (90.2%)	7,538,532 (88.4%)
*zip3*Δ sample 1	3,760,946	2,824,442 (75.1%)	ND	2,698,444 (71.7%)
*zip3*Δ sample 2	10,203,933	7,216,350 (70.7%)	ND	6,952,424 (68.1%)
*tel1*Δ *zip3*Δ sample 1	2,866,608	2,015,418 (70.3%)	ND	1,876,596 (65.5%)
*tel1*Δ *zip3*Δ sample 2	9,777,864	9,684,479 (99.0%)	8,638,972 (88.4%)	8,516,739 (87.1%)
Wild type (Chr III insert)	2,090,663	1,869,796 (89.4%)	805,308(38.5%)	780,524 (37.3%)
*tel1*Δ (Chr III insert)	3,127,825	2,956,817 (94.5%)	2672,189 (85.4%)	2,612,713 (83.5%)
Wild type (Chr IX insert)	81,020,056	76,396,867 (94.3%)	28,700,793 (35.4%)	27,770,451 (34.3%)
*tel1*Δ (Chr XI insert)	6,823,864	6,310,808 (92.5%)	5,610,186 (82.2%)	5,485,645 (80.4%)

[a] The fraction of sequences that could not be mapped likely reflect sequencing errors, adapter dimers, PCR dimers and bona fide Spo11-oligos derived from genomic regions that are unique to SK1 (i.e., not found in the S288C reference genome assembly).
[b] Total number of reads that filtered to remove reads with poor alignment and/or adapter clipping. ND, filtering not done.
[c] Total number of reads that mapped to only one position in the genome.

Table S2: Yeast strains

Strain No.	Genotype
SKY 3935	*MAT*α*; ho::LYS2; lys2; ura3; leu2::hisG; his3::hisG; SPO11-5ProA-his5*$^{+}_{sp}$
SKY 3934	*MAT*a*; ho::LYS2; lys2; ura3; leu2::hisG; his3::hisG; SPO11-5ProA-his5*$^{+}_{sp}$
SKY 3950	*MAT*a*; ho::LYS2; lys2; ura3; leu2::hisG; his3::hisG; SPO11-5ProA-his5*$^{+}_{sp}$*; tel1Δ::kanMX*
SKY 3951	*MATα; ho::LYS2; lys2; ura3; leu2::hisG; his3::hisG; SPO11-5ProA-his5*$^{+}_{sp}$*; tel1Δ::kanMX*
SKY 3952	*MATa, ho::LYS2; lys2; ura3; leu2::hisG; his3::hisG; SPO11-5ProA-his5*$^{+}_{sp}$*; tel1-kd-URA3*
SKY 3953	*MAT*α*, ho::LYS2; lys2; ura3; leu2::hisG; his3::hisG; SPO11-5ProA-his5*$^{+}_{sp}$*; tel1-kd-URA3*
SKY3954	*MAT*α*; ho::LYS2; lys2; ura3::pRS306-URA3; leu2::hisG; his3::hisG; SPO11-5ProA-his5*$^{+}_{sp}$
SKY 3967	*MAT a; ho::LYS2; lys2; LEU2; his3::hisG; ura3::pRS306-URA3; SPO11-5ProA-his5*$^{+}_{sp}$*; rec114::kanMX; REC114-NAT*
SKY 3968	*MAT*α*; ho::LYS2; lys2; LEU2; his3::hisG; ura3::pRS306-URA3; SPO11-5ProA-his5*$^{+}_{sp}$*; rec114::kanMX; REC114-NAT*
SKY 3955	*MATa, ho::LYS2; lys2, LEU2; his3::hisG; ura3::pRS306-URA3; SPO11-5ProA-his5*$^{+}_{sp}$*; rec114::kanMX; rec114-8A-NAT*
SKY 3956	*MAT*α *; ho::LYS2; lys2; LEU2; his3::hisG; ura3::pRS306-URA3; SPO11-5ProA-his5*$^{+}_{sp}$*; rec114::kanMX; rec114-8A-NAT*
SKY 3965	*MATa; ho::LYS2; lys2; LEU2; his3::hisG; ura3::pRS306-URA3; SPO11-5ProA-his5*$^{+}_{sp}$
SKY 3966	*MAT*α*; ho::LYS2; lys2; LEU2; his3::hisG; ura3::pRS306-URA3; SPO11-5ProA-his5*$^{+}_{sp}$
SKY 3957	*MATa; ho::LYS2; lys2; ura3; leu2::hisG; his3::hisG; hop1::LEU2; hop1SCD-URA3; SPO11-5ProA-his5*$^{+}_{sp}$*; rec114::KANMX; rec114-8A-NAT*
SKY 3958	*MAT*α*; ho::LYS2; lys2; ura3; leu2::hisG; his3::hisG; hop1::LEU2; hop1SCD-URA3; SPO11-5ProA-his5*$^{+}_{sp}$*; rec114::KANMX; rec114-8A-NAT*
SKY 3959	*MAT*a*; ho::LYS2; lys2; ura3; leu2::hisG; his3::hisG; SPO11-5ProA-his5*$^{+}_{sp}$*; tel1Δ::kanMX*
SKY 3960	*MATα; ho::LYS2; lys2; ura3; leu2::hisG; his3::hisG; SPO11-5ProA-his5*$^{+}_{sp}$*; zip3Δ::hphMX; tel1Δ::kanMX*
SKY 3936	*MATa; ho::LYS2; lys2; ura3; leu2::hisG; his3::hisG; SPO11-5ProA-his5*$^{+}_{sp}$*; zip3Δ::hphMX*
SKY 3937	*MATα; ho::LYS2; lys2; ura3; leu2::hisG; his3::hisG; SPO11-5ProA-his5*$^{+}_{sp}$*; zip3Δ::hphMX*
SKY 3961	*MAT a/α; ho::LYS2/"; lys2/", ura3/"; leu2::hisG/"; his4:: pMJ113-URA3/"; SPO11-5ProA-his5*$^{+}_{sp}$*/"*
SKY 3962	*MAT a/α; ho::LYS2/"; lys2/"; ura3/"; leu2::hisG/"; his4::pMJ113-URA3/"; SPO11-5ProA-his5*$^{+}_{sp}$*/"; tel1::kanMX/"*
SKY 3963	*MAT a/α; ho::LYS2/"; lys2/"; ura3/"; leu2::hisG/"; por2::arg-Nsp-URA3/"; SPO11-5ProA-his5*$^{+}_{sp}$*/"*
SKY 3964	*MAT a/α; ho::LYS2/"; lys2/"; ura3/"; leu2::hisG/"; por2::arg-Nsp-URA3/"; SPO11-5ProA-his5*$^{+}_{sp}$*/"; tel1::kanMX/"*

SPO11-5ProA-his5$^{+}_{sp}$ is *SPO11* tagged at its 3′ end with 5 copies of coding sequence for a protein A tag and marked with the *Schizosaccharomyces pombe his5*$^{+}$ gene, which complements the *S. cerevisiae his3* mutation.